Soil Bin and Field Tests of an On-The-Go Soil Strength Profile Sensor

S. O. Chung, K. A. Sudduth, C. Plouffe, N. R. Kitchen

Abstract. *An on-the-go soil strength profile sensor (SSPS) was previously developed to measure the within-field spatial variability in soil strength at five evenly spaced depths up to 50 cm. In this article, performance of the SSPS was evaluated using soil bin and field data. First, the SSPS was tested in a soil bin at different depths (10, 20, and 30 cm), forward speeds (from 0.5 to 3.0 m s^{-1}), and compaction levels (high and low). Second, data were collected in two fields having variable soil texture, bulk density, and water content. Prismatic soil strength index (PSSI, defined as force divided by the base area of the horizontally operating prismatic tip) and penetrometer cone index were measured at five depths (10, 20, 30, 40, and 50 cm) across entire fields and also more intensively in four 10 × 10 m areas selected for soil texture differences. Auxiliary data collected were soil bulk density, soil water content, and apparent soil electrical conductivity (EC_a). When the SSPS was tested in the soil bin, increases in PSSI with speed were less than 15% from 0.5 to 3.0 m s^{-1} operating speed. Based on soil bin results, we selected 1.5 m s^{-1} as a maximum field data collection speed, below which speed effects on PSSI were deemed negligible. Mean PSSI values collected in adjacent, parallel transects were not statistically different, confirming the repeatability and stability of soil strength sensing with the SSPS. Field data showed that, in general, PSSI was higher at locations with lower EC_a, lower water content, and greater bulk density. Results of stepwise multiple linear regression showed that variability in PSSI was better explained when interactions among the soil variables were included as independent variables and when data were grouped into subsets by depth and/or EC_a level. Over entire fields, R^2 values for estimating PSSI were 0.66 and 0.61 for a claypan soil field and a flood plain field, respectively. These results will be useful for interpreting PSSI and for future applications of the SSPS in crop management, e.g., delineation of highly compacted within-field areas and control of variable tillage operations.*

Keywords. *Cone index, Cone penetrometer, Precision agriculture, Sensor, Soil bin, Soil compaction, Soil strength.*

Soil compaction caused by wheel traffic of large agricultural machinery and/or tillage operations, as well as due to natural phenomena, is a concern in crop production and the environment. When soil is compacted, soil physical properties, which play an important role in growth and development of plants, are negatively altered. Soil compaction has deleterious effects on crop growing conditions and the environment (Soane and Van Ouwerkerk, 1994), effects which are difficult to remedy. The causes of soil compaction and the resulting soil deformations may be different in the various soil layers (i.e., top layer, arable layer, and subsoil) (Koolen and Kuipers, 1983).

An approach to quantifying soil compaction is to measure soil strength, since soil strength is strongly associated with compactness and drainable porosity (Canarache, 1991). The cone penetrometer has been the tool of choice for quantifying soil strength *in situ* (Mulqueen et al., 1977). The index of soil strength measured by a cone penetrometer, cone index (CI), is defined as the force per unit base area required to push the penetrometer through a specified small increment of depth (*ASABE Standards*, 2005a, 2005b). Since readings are taken vertically starting at the soil surface, cone penetrometer readings require a "stop-and-go" procedure with data collected at discrete locations. Because of this, it would be laborious and time-consuming to collect enough data with a cone penetrometer to accurately map compaction variations within a field.

To overcome this limitation of the penetrometer, a number of researchers have attempted "on-the-go" measurement of soil strength. These approaches have differed in: (1) the type of soil strength measured: tillage draft (Van Bergeijk et al., 2001), bending stress on a tine (Adamchuk et al., 2001), and "CI-like" soil resistance experienced by a soil-penetrating tip (Andrade-Sanchez et al., 2007); (2) the number of sensing elements: single (Alihamsyah et al., 1990) and multiple (Chukwu and Bowers, 2005); and (3) the shape and extension of sensing tips: 60° prismatic tip extended from a main blade (Chung et al., 2006) and 30° prismatic flush-mounted tip (Hall and Raper, 2005).

Submitted for review in October 2006 as manuscript number PM 6720; approved for publication by the Power & Machinery Division of ASABE in January 2008. Presented at the 2004 ASABE Annual Meeting as Paper No. 041039.

Mention of trade names or commercial products is solely for the purpose of providing specific information and does not imply recommendation or endorsement by Chungnam National University, the USDA, or Deere & Company.

The authors are **Sun-Ok Chung, ASABE Member Engineer,** Full-Time Instructor, Department of Bioindustrial Machinery Engineering, Chungnam National University, Daejeon, Korea; **Kenneth A. Sudduth, ASABE Fellow,** Agricultural Engineer, USDA-ARS Cropping Systems and Water Quality Research Unit, Columbia, Missouri; **Carol Plouffe, ASABE Member Engineer,** Soil and Crop Systems Engineer, Deere & Company Moline Technology Innovation Center, Moline, Illinois; and **Newell R. Kitchen,** Soil Scientist, USDA-ARS Cropping Systems and Water Quality Research Unit, Columbia, Missouri. **Corresponding author:** Kenneth A. Sudduth, USDA-ARS Cropping Systems and Water Quality Research Unit, 269 Agricultural Engineering Bldg., University of Missouri, Columbia, MO 65211; phone: 573-882-4090; fax: 573-882-1115; e-mail: Ken.Sudduth@ ars.usda.gov.

Factors affecting soil strength have been identified by analytical models (Hettiaratchi and Reece, 1974), semi-empirical techniques like dimensional analysis (Schuring and Emori, 1964; Wismer and Luth, 1972), and experimental study (Alihamsyah et al., 1990). The factors generally fall into five categories: (1) soil condition, e.g., bulk density, water content, texture, internal friction angle, and cohesion; (2) operating consideration, e.g., speed and depth of operation, and direction of movement (horizontal vs. vertical); (3) tool design, e.g., geometry and surface roughness; (4) soil-tool interaction, e.g., friction angle and adhesion; and (5) load distribution on the soil surface. In addition to individual effects of the factors, interactions among the factors also affect soil strength.

Previous research showed that major soil properties affecting soil strength were water content, bulk density, and particle size distribution (i.e., clay content) (Perumpral, 1987; Elbanna and Witney, 1987; Guerif, 1994). In performance evaluation of a rigid tine, Stafford (1979) found that water content was the primary factor determining soil forces, and soil type only affected soil forces secondarily in that texture affected the pertinent range of soil water content. Perumpral (1987) stated that cone index increased with increasing soil density and decreasing soil water content. Ayers and Perumpral (1982) developed an equation for cone index as a function of soil water content and density for five different soil types. They concluded that the specific water content for maximum soil strength depended on the soil type and increased as the percentage of clay increased. Elbanna and Witney (1987) expressed cone penetration resistance at an average tillage depth as a function of clay fraction, cohesive and frictional coefficients, soil water content, and soil specific weight. Wells and Treesuwan (1978) investigated the response of various soil strength indices to changing water content and bulk density. They also found that soil bulk density and water content exhibited discernable effects on cone index, soil deformation, and soil internal friction angle. Zhang et al. (2001) explained the changes in soil shear strength parameters due to changes in bulk density and soil water content with the Mohr-Coulomb failure equation and the principles of effective stress for unsaturated soils. Plasse et al. (1985) stated that soil cohesion and adhesion were major contributors to draft force and were very dependent on soil water status.

An important operational factor affecting soil strength measurement is vehicle forward speed for narrow tines moving horizontally (e.g., an on-the-go soil strength sensor) and penetration rate for tools operating vertically (i.e., cone penetrometer). High speeds near those encountered in normal tillage operations may result in a significant force increase. McKyes (1985) discussed two dynamic effects: inertia forces due to accelerating the soil volume, and changes in soil strength at a high rate of shear. He also stated that the effect of shear rate was not significant in purely frictional soils, but was significant in clay soils, outweighing the inertia forces. It is generally accepted that the soil force acting on a tool body increases approximately with the square of speed (Stafford, 1979; Wheeler and Godwin, 1996). Schuring and Emori (1964) found a critical speed (v), below which the effects of operating speed would not be significant, as a function of acceleration of gravity (g) and tool width (b). The critical speed was expressed as $v = (5gb)^{0.5}$, based on the results of dimensional analysis.

Operating depth also affects soil strength due to differences in soil conditions and the soil failure mechanism along the soil profile. Sojka et al. (2001) related cone index to water content and bulk density of a silt loam soil. The relationship was poor when derived from full-profile data sets but improved when data were segregated by depth. The authors attributed this to differences in bulk density and texture with depth. Luth and Wismer (1971) tested flat soil cutting blades in sand, finding that horizontal force increased as approximately the square of depth for blades of 2.5 to 12.6 cm width. In a saturated clay soil (Wismer and Luth, 1972), force was related to depth by a power less than or equal to one for the same range of blade widths. Glancey et al. (1989) developed an instrumented chisel using multiple strain gauges to predict tillage implement draft requirements. Field experiments were conducted at two operating depths (15 and 30 cm) in two soil conditions (tilled and untilled). Force distribution over the tillage depth was linear at the shallow operating depth in both soils, while it was nonlinear at the greater operating depth in the untilled soil.

The literature shows that soil conditions and operational considerations are factors significantly affecting soil strength, and these factors interact in a complex manner. Therefore, evaluation of an on-the-go soil strength sensor in various soil and operating conditions is important for better understanding of the strength measurements obtained by a sensor.

Objectives

The overall objective of this research was to evaluate the performance of our previously developed soil strength profile sensor (Chung et al., 2006) under different soil and operating conditions. Specific objectives were:

- Test the sensor in an indoor soil bin to investigate the effects of operating speed on soil strength measurements, and to determine optimum operating speed for field data collection.
- Test the sensor in fields having variations in bulk density, water content, and soil texture to evaluate its repeatability and overall performance in mapping spatial and vertical variations in soil strength.
- Relate sensor field measurements of soil strength to soil properties such as bulk density, water content, and soil texture, and also to soil strength parameters such as shear stress, cohesion, and internal friction angle determined by laboratory tests.

Materials and Methods

Soil Strength Profile Sensor

Our previously developed soil strength profile sensor (SSPS) was used to collect data in a soil bin and two research fields. The SSPS, configured with five prismatic force-sensing tips on a 10 cm depth increment and extended 5.1 cm ahead of a main blade, provided a soil strength profile to a depth of 50 cm. The soil force on each tip was measured by a load cell located in the main blade and in contact with the rear end of the tip shaft. Force measured by the SSPS divided by the base area of the sensing tip was defined as the prismatic soil strength index (PSSI, MPa), comparable to the

CI of a vertically operating cone penetrometer. Additional details of the SSPS design are given in Chung et al. (2006).

Soil Bin Tests

Effects of operating speed on PSSI were investigated in an indoor soil bin located at the John Deere Soil Dynamics Laboratory (Moline, Ill.). This facility provided homogeneous soil conditions and better control of operating speed than in typical field operation. The soil bin was 33 m long (14 m of soil) by 1.6 m wide and 0.85 m deep. The soil in the bin was 15% clay, 35% silt, and 50% sand, and soil water content was held constant to within 1% during the tests. Different levels of compaction were achieved by adjusting the pressure of a compaction roller.

Two kinds of experiments were conducted in the soil bin: acceleration tests and fixed speed tests. First, acceleration tests were implemented to see if any correction of sensor measurements as a function of speed might be necessary for data collected under field conditions, where operating speed would continuously change. Speed was changed from 0.5 to 3.0 m s^{-1} as a linear function of sensor position as it moved through the bin. The tests were conducted at two compaction levels with three replications, resulting in a total of six passes. Second, PSSI data were collected at two compaction levels (low and high pressure settings of the compaction roller) and three constant speeds (0.5, 1.5, and 2.5 m s^{-1}).

In the soil bin tests, PSSI data were collected at three depths (10, 20, and 30 cm) at a 100 Hz sampling frequency. An additional load cell covered with aluminum foil was placed outside of the main blade of the sensor to act as a reference load cell and detect potential electrical noise from the environment. Prior to each SSPS run, two CI profiles were obtained to a 40 cm depth using a large cone penetrometer (*ASABE Standards*, 2005a) at a 30 mm s^{-1} penetration rate, one in the first half and the other in the second half of the soil bin. The low and high roller pressure settings used in these experiments provided nominal CI values near the soil surface of 0.55 MPa and 0.99 MPa, respectively, and held these levels nearly constant along the length of the soil bin. However, CI varied considerably both laterally across the soil bin (mean CV = 4% at 10 and 20 cm depths; mean CV = 34% at 30 cm depth) and by depth (mean CV = 25%) and was also somewhat different between soil preparations (mean CV = 8%). Therefore, the locations of the CI sampling and SSPS passes were carefully synchronized, and the CI sampling was done in the path of, and prior to, the SSPS passes. After all tests were completed, the soil was prepared again, and 7 cm diameter, 5 cm long soil core samples were obtained centered at the three depths where PSSI was measured (10, 20, and 30 cm) at four locations in each compaction regime. For these 24 samples, dry bulk density and gravimetric water content were determined.

Output signals from the SSPS load cells and the cone penetrometer were recorded by a data acquisition system mounted on the soil bin tool carriage. To remove small-scale variability and obtain more reliable PSSI and CI measurements, both signals were averaged. A 5 cm depth-averaged CI was calculated centered on each of the three tip depths (10, 20, and 30 cm). For the acceleration tests, average PSSI was calculated on a 0.2 m s^{-1} interval from 0.5 to 2.9 m s^{-1}, resulting in 12 data points for each pass, or a total of 216 values (12 points × 3 replications × 2 compaction levels × 3 depths). For the fixed speed tests (0.5, 1.5, and 2.5 m s^{-1}), 2 m distance-averaged PSSIs were calculated.

Field Test Sites

The performance of the SSPS was also evaluated at two research sites (fig. 1): site 1 (13.5 ha) near Centralia, Missouri (39.230° N, 92.117° W) and site 2 (4.5 ha) near Hartsburg, Missouri (38.753° N, 92.384° W). These sites, located within

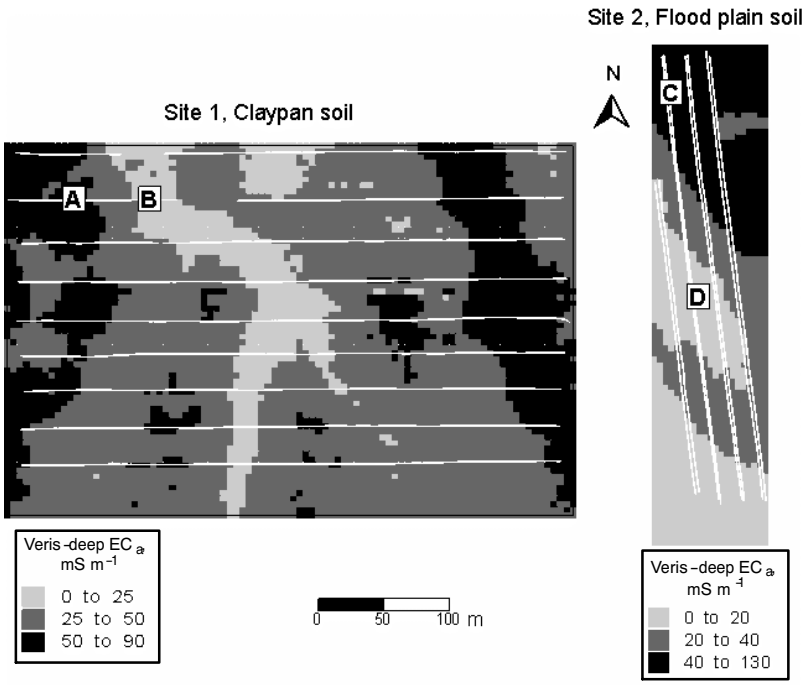

Figure 1. Field data collection scheme overlaid on Veris-deep EC_a maps. PSSI data collection (white lines) was done on 20 to 30 m transect spacings. Paired transects at site 2 were used to evaluate repeatability of PSSI measurements. Four small 10 × 10 m areas (A, B, C, and D), each comprising a relatively homogeneous soil texture, were chosen for intensive data collection.

fields managed in corn-soybean rotations, were chosen because our previous research (e.g., Kitchen et al., 1999; Sudduth et al., 2003) identified them as having well-defined patterns of soil spatial variability. The soils found at site 1 were of the Mexico series (fine, smectitic, mesic aeric Vertic Epiaqualfs) and the Adco series (fine, smectitic, mesic aeric Vertic Albaqualfs). Surface textures of these somewhat poorly drained soils ranged from silt loam to silty clay loam. The subsoil claypan horizon(s) were silty clay loam, silty clay, or clay, and commonly contained as much as 50% to 60% smectitic clay. Topsoil depth above the claypan (depth to the first Bt horizon) ranged from less than 10 cm to greater than 100 cm (Sudduth et al., 2003). The alluvial soils at site 2 in the Missouri River flood plain were mostly of the Leta series (clayey over loamy, smectitic, mesic Fluvaquentic Hapludolls) and Haynie series (clayey over loamy, smectitic, mesic Fluvaquentic Hapludolls). A few areas within this field site had no soil series name assigned but were classified as being "sand over sand." These sand depositional areas resulted from flooding in 1993 when the Missouri River levees failed.

Field Data Collection

PSSI data at five depths (10, 20, 30, 40, and 50 cm) were collected with the SSPS on a 30 m transect spacing for site 1 (21 Oct. 2003; fig. 1, left) and on a 20 m transect spacing for site 2 (22 Oct. 2003; fig. 1, right). The direction of the PSSI collection was slightly angled (about 5˚) with respect to the crop row to minimize effects of possible systematic patterns of soil strength due to past crop and field management practices. The nominal operating speed of the tractor-mounted SSPS was 1.5 m s^{-1} and the data sampling rate was 10 Hz. Additional transects (test transects) were made with the SSPS in the opposite direction of travel and parallel to the first set of transects (reference transects) at site 2 to evaluate repeatability of the PSSI measurements. Distances between the reference and test transects were less than 3 m, but no closer than 1 m.

On a 30 m interval along each transect, triplicate CI profiles were obtained with an ASAE-standard small cone penetrometer, and averaged to a single profile at each location (133 locations at site 1 and 52 locations at site 2). A non-standard penetration rate of 40 mm s^{-1} was used to speed data collection and because our previous research (Sudduth et al., 2004) showed no significant difference between this rate and the standard 30 mm s^{-1}. The CI data were obtained an average of 1.5 m away from the PSSI transects, to avoid possible effects of SSPS soil disturbance and tractor wheel-track compaction. At every second CI collection location (52 locations at site 1 and 25 locations at site 2), 4 cm diameter soil cores were obtained and segmented into five 10 cm long depth intervals centered on the PSSI measurements (i.e., 5 to 15 cm, 15 to 25 cm, 25 to 35 cm, 35 to 45 cm, 45 to 55 cm) for gravimetric determination of dry bulk density and soil water content. Positional information for CI, PSSI, and soil sampling was collected using a DGPS receiver with an accuracy of 1 m or better.

Apparent soil electrical conductivity (EC_a) data were measured with a Veris Model 3100 sensor on transects parallel to PSSI data collection. Transects were 10 m apart, and EC_a data were obtained at a 4 to 6 m spacing along each transect. EC_a measurements are primarily dependent on soil texture and soil water content in non-saline soils, and have been used to differentiate soil types (Anderson-Cook et al., 2002) and soil conditions (e.g., bulk density and clay fraction; Johnson et al., 2001). Sudduth et al. (2003, 2005) investigated the relationship of EC_a to a number of soil properties over multiple fields in the north-central U.S., including one of the fields used in this study. They found that soil clay fraction and cation exchange capacity, another measurement strongly related to soil texture, were the two soil properties having the strongest effect on EC_a, Higher EC_a values indicated greater soil clay fractions (or smaller sand fractions) compared to low EC_a values (Sudduth et al., 2003). Therefore, we used EC_a as an indicator of soil textural differences within the field sites, grouping each site into three textural classes. Corresponding low, medium, and high EC_a ranges were 0-25, 25-50, and 50-76 mS m^{-1} for site 1, and 0-20, 20-40, and 40-81 mS m^{-1} for site 2 (fig. 1).

Four small (10 × 10 m) areas with relatively homogeneous soil textures were selected for more intensive data collection (fig. 1). The two areas selected in the Centralia field included relatively more clay (area A) and relatively more silt (area B) in the soil profile, while the areas in the Hartsburg field contained relatively more sand (area C) and relatively less sand (area D). In the small areas, five or six passes of PSSI data were collected on a 2 m transect spacing with a 100 Hz sampling rate. Triplicate CI profiles were obtained at 20 locations equally spaced within each area. Also within each area, four 7.6 cm diameter, 60 cm long undisturbed soil samples were obtained for laboratory tests and stored in a cold room at 4°C. Before testing, the samples were divided into 10 cm long increments corresponding to the five depths at which PSSI data were collected. Soil properties determined on these samples were dry bulk density and gravimetric water content, texture using the pipette method (Gee and Or, 2002), and cohesion (c) and internal friction angle (ϕ) using direct shear tests (Fredlund and Vanapalli, 2002). Soil-metal friction angle (δ) was calculated by $\delta = [(0.590 \times \text{sand fraction}) + (0.735 \times \text{silt fraction}) + (0.375 \times \text{clay fraction})] \times \phi$, where the coefficients were interpolated from Potyondy (1961) for unsaturated dense sand, silt, and clay soils, respectively. Adhesion (c_a) was calculated by $c_a = c(\cot\phi/\cot\delta)$, as suggested by Hettiaratchi and Reece (1967). Complete procedures used for soil property determination were described by Chung (2004).

Field Data Processing and Analysis

Field data collected by the SSPS required preprocessing. The raw data contained sections where the sensor was lifted from the ground on the tractor hitch, primarily at the beginning and end of each transect. This issue was resolved by removing data points where the PSSI values at 30, 40, and 50 cm depths were less than a threshold value of 0.5 MPa. Position data were corrected considering the direction of travel and the offset between the DGPS antenna and the strength sensor. PSSIs within small distances were averaged to obtain more reliable measurements for further non-spatial analyses. The averaging distance used was determined by examining the range of spatial dependency obtained through variogram analysis (Webster and Oliver, 1990).

The repeatability of soil strength measurements obtained with the SSPS was evaluated by comparing PSSI measurements obtained from the test transects at site 2 with those from the corresponding reference transects. At each CI data collection location, PSSI measurements were extracted

from the reference transect and the test transect such that the distances between the CI and PSSI locations were at a minimum. Then, PSSI data within the averaging distance determined from variogram analysis were averaged to allow a more reliable comparison. This approach was applied to the PSSI data for each sensing depth, resulting in a total of 260 PSSI data pairs.

Relationships between PSSI and soil properties were investigated using data from (1) the four 10 × 10 m areas and (2) the two entire field sites. In each of the small areas, mean PSSI was determined for each depth. Thus, a total of 20 observations, each consisting of mean PSSI, dry bulk density, water content, texture, cohesion, internal friction angle, adhesion, and soil-metal friction angle, were used for analyses. For the entire sites, PSSI was compared with bulk density and water content obtained from soil samples, and with Veris deep EC_a. At each CI data collection location, distance-averaged PSSI at each of five depths was calculated as described above. Five-centimeter depth-averaged CI data were calculated centered on each PSSI measurement depth. Corresponding EC_a data were obtained from the nearest grid cell based on 5 × 5 m kriging.

Spatial and non-spatial statistical methods were applied to analyze the data. To determine optimum distance for PSSI averaging and grid size for mapping, variogram analysis was conducted using S+SpatialStats version 1.5 (MathSoft, Inc., Seattle, Wash.), and mapping was done using Surfer version 8.0 (Golden Software, Inc., Golden, Colo.). PSSI measurements were plotted against CI, EC_a, bulk density, and soil water content. These scatter plots were visually investigated to identify possible outliers for removal before statistical analysis. Visual examination of the data was also used to identify candidate functional relationships between PSSI and the other variables and to evaluate the possible need for grouping the data (e.g., by depth or EC_a class). Multiple linear regression was applied to predict PSSI as a function of the other variables. The independent variables of CI, EC_a, bulk density, and soil water content, along with all quadratic and two-variable interaction terms, were candidates for inclusion in the model. For non-spatial statistics, procedures in SAS version 8.01 (SAS Institute, Inc., Cary, N.C.) were used: analysis of variance (GLM), Duncan's multiple range tests (MEANS), correlation analysis (CORR), and regression analysis (REG). To reduce the issues associated with multicollinearity among the variables in regression analysis and to enhance reliability of the models, the stepwise option was used with variable entry and removal levels of 0.15 for variable selection.

Results and Discussion

Effects of Operating Speed

Figure 2 shows an example of results of the on-the-go acceleration tests in the soil bin. Throughout the tests, output from the reference load cell was quite consistent, so no compensation was applied to outputs from the test load cells. Generally, PSSI was higher at greater depths and higher compaction levels (or CI values). PSSI increased slightly as speed increased linearly from 0.5 to 3.0 m s^{-1}. An exception to this was the localized decrease in PSSI where CI measurements were obtained in the path of the SSPS prior to the passes (fig. 2). In an analysis of variance, compaction (2 levels) and sensor tip operating depth (3 levels) explained 94% of the variability in PSSI, and both variables were highly significant ($P < 0.001$). Thus, speed effects were investigated separately within each compaction-depth combination.

Scatter plots of PSSI vs. speed level (fig. 3) showed that the speed effects on PSSI were more pronounced at the high compaction setting. This pattern was consistent within each measurement depth (i.e., 10, 20, and 30 cm). When data from three replications were averaged, relative PSSI increases from the lowest speed level (0.6 m s^{-1}) to the highest (2.8 m s^{-1}) were less than 14% within each compaction setting at the 20 and 30 cm depths. Relative increases in PSSI were greater at the 10 cm depth, but absolute increases remained less than 0.15 MPa. When data were averaged across all depths and compaction levels to focus on the speed effects, increases in the average PSSI relative to that at the lowest speed level were less than 10% at speeds less than 2.0 m s^{-1} (fig. 4).

Fixed speed tests showed similar trends (fig. 4), although direct comparison of these results with those for on-the-go acceleration tests was not be possible since levels of

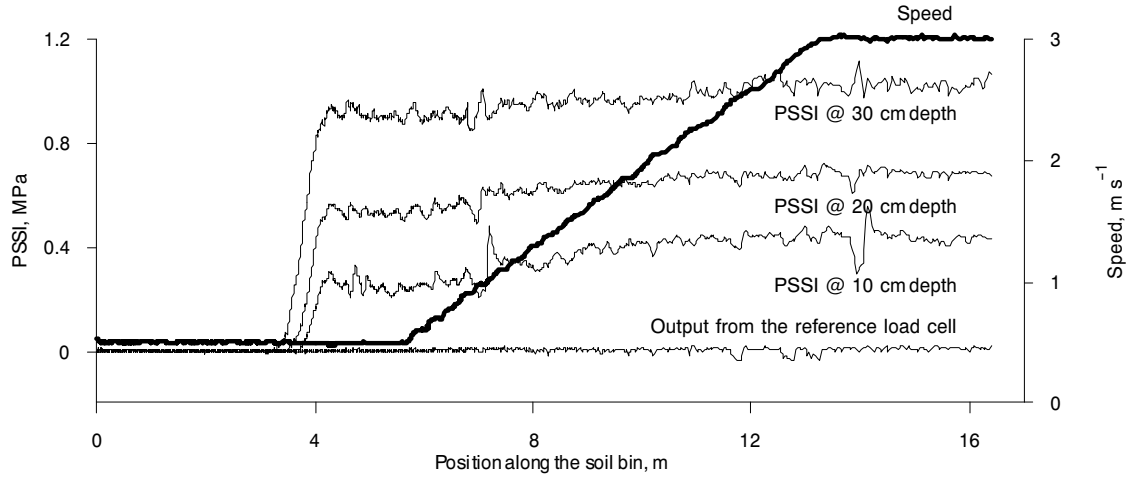

Figure 2. Example of acceleration test results from the soil bin. Speed was changed from 0.5 to 3.0 m s^{-1} as a linear function of distance along the soil bin. CI data were collected prior to the sensor runs at approximately 7 and 14 m, and the effects of the resulting soil disturbance can be seen in the PSSI data. The shank engaged the soil at approximately 4 m.

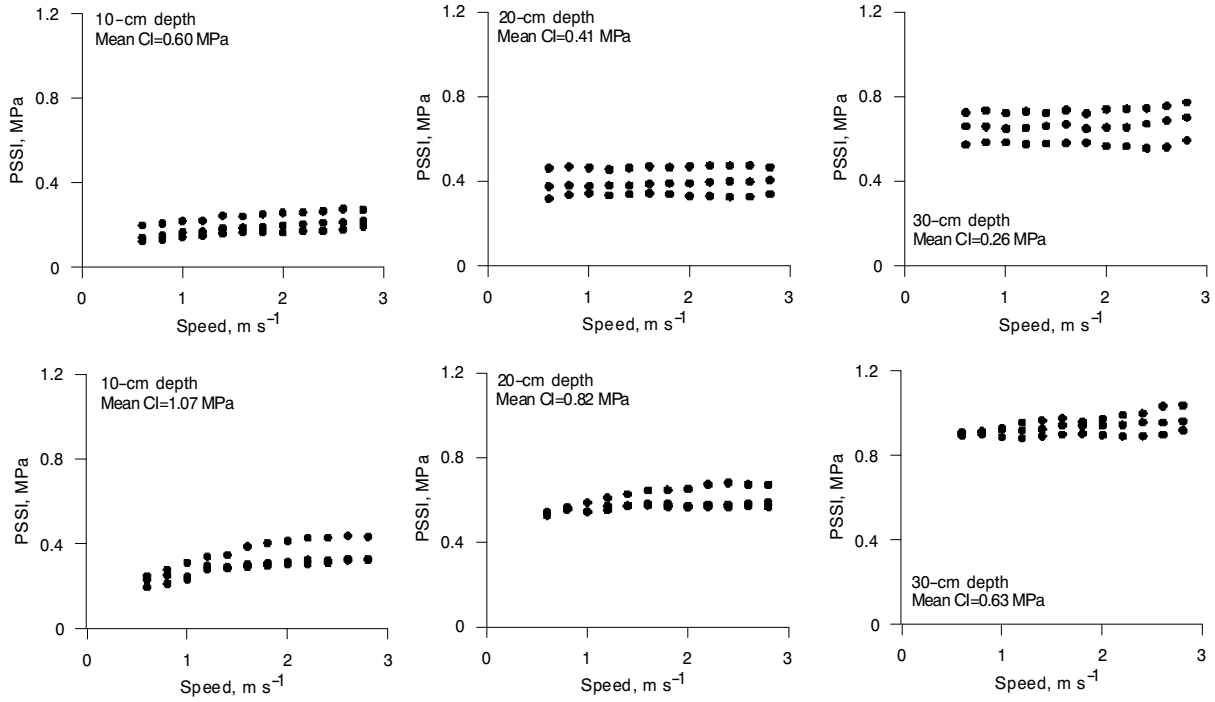

Figure 3. Plots of 0.2 m s^{-1}-averaged PSSI vs. speed level at 10 cm (left), 20 cm (center), and 30 cm (right) depths and low (top) and high (bottom) soil bin compaction settings.

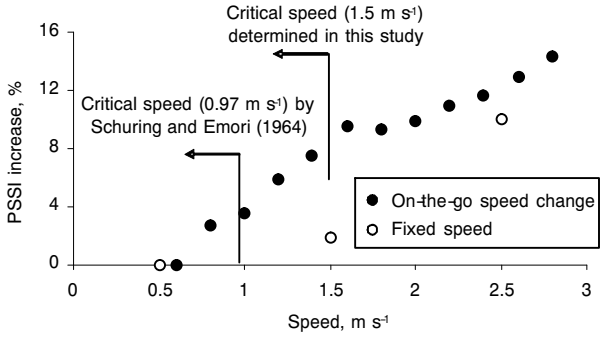

Figure 4. Increase in 0.2 m s^{-1} averaged PSSI for the acceleration (on-the-go speed change) and fixed speed tests conducted in the soil bin.

compaction measured as CI were different and the PSSI ranges obtained were also different. Analysis of variance using compaction (2 levels), operating depth (3 levels), and speed (3 levels) as class variables explained 95% of the PSSI variability in the fixed speed tests, and the effects of all independent variables were highly significant ($P < 0.001$). Duncan's multiple range test showed that PSSI means at different depths (0.19 MPa at 10 cm, 0.37 MPa at 20 cm, 0.61 MPa at 30 cm) and compaction levels (0.34 MPa at low compaction, 0.44 MPa at high compaction) were significantly different ($\alpha = 0.05$). When increases in PSSI relative to PSSI at the minimum tested speed of 0.5 m s^{-1} were calculated, there was a 2% increase in PSSI at 1.5 m s^{-1}, which was not significant ($\alpha = 0.05$). The approximately 10% increase in PSSI at 2.5 m s^{-1} was significant ($\alpha = 0.05$).

In one previous study, Glancey et al. (1996) found that the effect of speed was negligible for five different implements at speeds less than 2.0 m s^{-1}. Using the method proposed by Schuring and Emori (1964), however, the calculated critical speed for the SSPS was 0.97 m s^{-1}. This calculated critical speed was relative to quasi-static operation, while the minimum operation speed used for comparison in our tests was 0.5 m s^{-1}. From these results, we selected 1.5 m s^{-1} as the maximum field operating speed. Field PSSI data were collected over a narrow speed range at approximately 1.5 m s^{-1}.

Processing and Mapping Field PSSI Data

Field PSSI measurements showed variations in soil strength at different within-field locations as well as at different tip depths. The field PSSI data contained both high-frequency (short-scale) components and underlying low-frequency (long-scale) components. High-frequency components are often due to measurement system error and/or micro-variability over small distances (e.g., periodic development of the soil failure zone). Although it would be important to retain these high-frequency data for some analyses, we averaged the PSSI data to obtain more reliable measurements for comparison with other variables measured

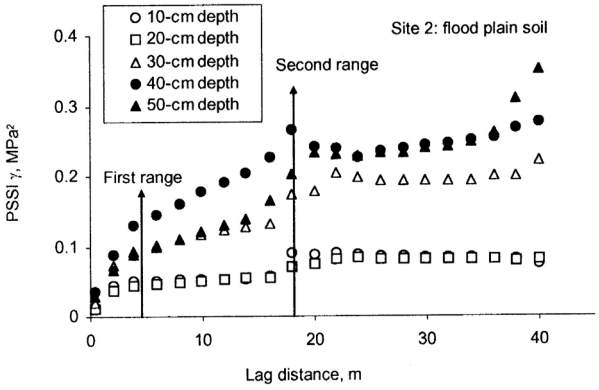

Figure 5. Experimental variograms for PSSI measurements at the five tip depths at site 2.

at discrete locations (e.g., CI, soil water content). Variogram analysis (Chung, 2004) identified two ranges of spatial dependence for both sites: one at distances between 4 and 6 m due to the variability within transects, and the other at distances similar to the transect spacing (fig. 5). Based on this analysis, we selected 4 m as the distance over which to average PSSI within transects. About 27 data points were used to calculate each 4 m averaged PSSI value for further non-spatial analyses, considering the approximately 1.5 m s^{-1} operating speed and 10 Hz sampling rate. This averaging window size (27 points or 4 m) was similar to that used by Lui et al. (1996), who averaged 40 data points over 3 m to obtain a reliable local draft value for a 16 mm wide shank.

As an optimum grid size for PSSI mapping, we selected an intermediate value of the first and second variogram ranges, or 10 m. For Veris-deep EC_a, we selected a 5 m grid size for mapping, since the EC_a variograms showed a range of approximately 5 m for both sites (Chung, 2004). Additionally, use of this smaller grid for the EC_a data allowed more accurate matching of EC_a to individual PSSI data for subsequent statistical analysis. Figure 6 shows the resulting kriged maps of PSSI at the five sensing depths and Veris-deep

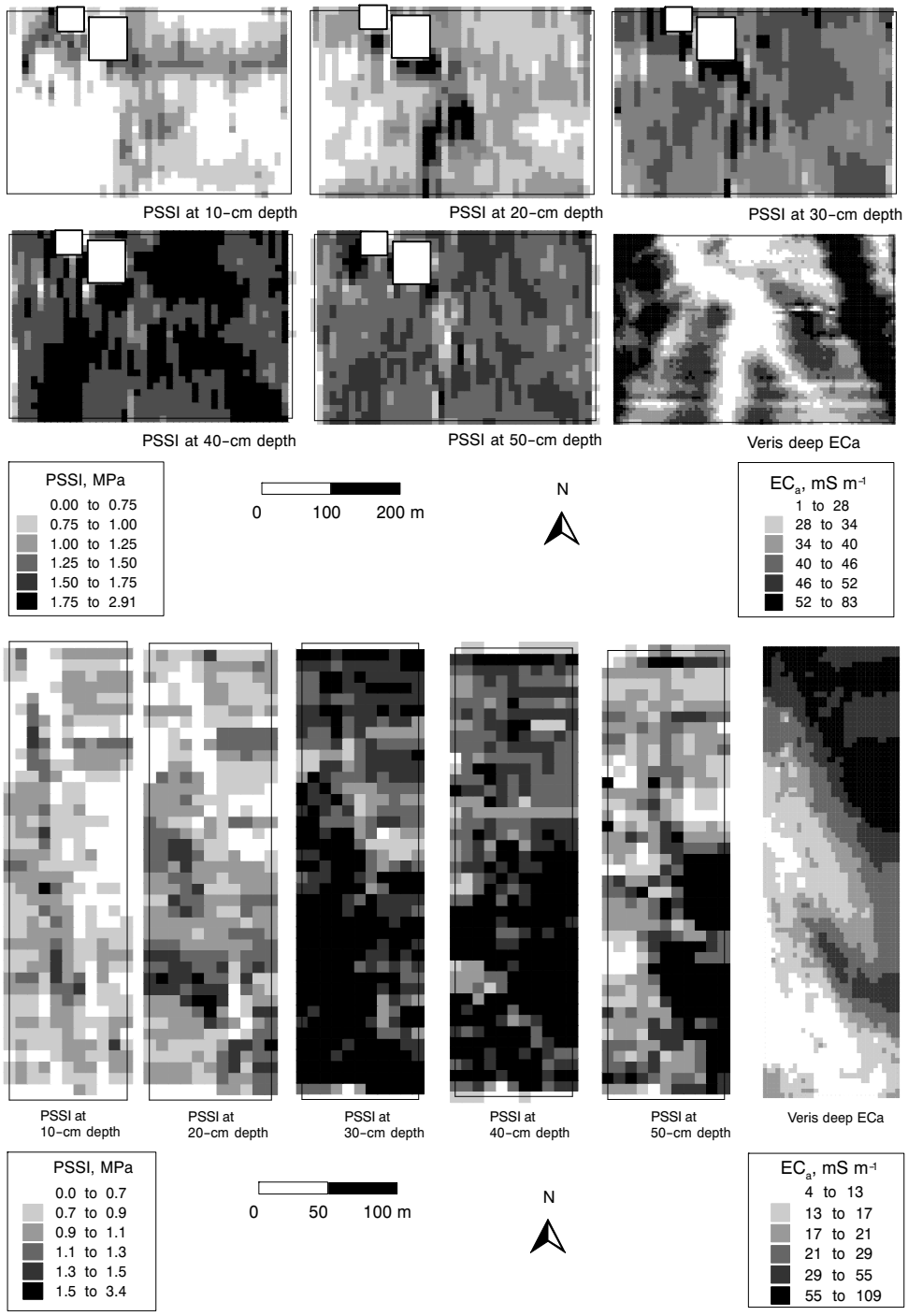

Figure 6. Kriged maps of PSSI (10 × 10 m grid) at the five sensing depths and Veris-deep EC_a (5 × 5 m grid) for site 1 (top) and site 2 (bottom). White squares in PSSI maps for site 1 are areas of missing data due to incomplete transects.

EC_a for sites 1 (top) and 2 (bottom). Compared with the EC_a maps, the PSSI maps exhibited coarser spatial patterns due to the greater transect spacings used in data collection. Patterns in the PSSI maps for site 1 were elongated in the north-south direction, an artifact of the difference between the transect spacing (30 m) and the grid size for the kriging (10 m). Compared with the EC_a map, the overall pattern of PSSI indicated that soil strength was higher in areas of lower EC_a, corresponding to lower soil clay fractions. A similar pattern was seen at all depths, but the degree of correspondence between the PSSI and EC_a maps was somewhat different for different depths. The overall pattern of higher PSSIs in low EC_a areas and the different degrees of similarity between the PSSI and EC_a maps at different depths were also found in site 2. The correlation of PSSI to EC_a was strongest at the 20 cm depth for both sites (r = -0.49 for site 1, and r = -0.51 for site 2).

PSSI was highest at the 40 cm depth for both sites. Taylor and Gardner (1963) stated that CI readings above 2 MPa could significantly impede root growth. When this criterion was applied to the 40 cm depth PSSI maps, cells where PSSI was greater than 2 MPa were 4.9% and 15.8% of the total number of cells for sites 1 and 2, respectively. Based on this criterion and data, soil strength in most areas of these two fields should not be limiting to growth of crop roots.

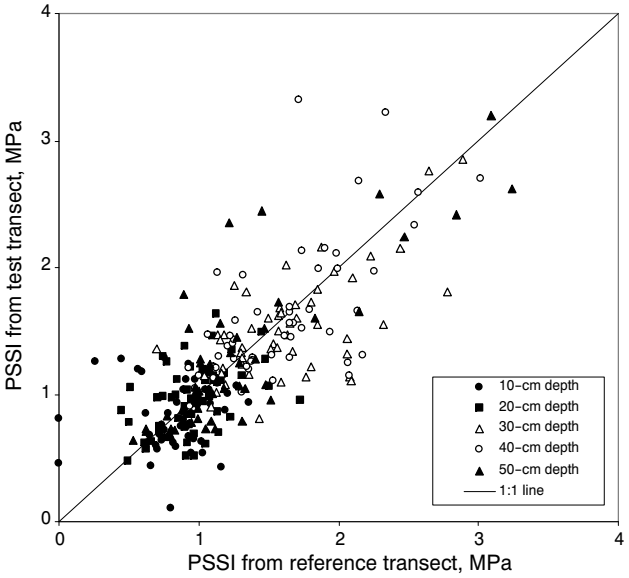

Figure 7. Comparison of PSSI obtained from reference and test transects at site 2.

Repeatability of Soil Strength Sensing

The 4 m averaged PSSI values from the test transects were linearly related to those from the reference transects (fig. 7). The central tendency of the relationship was close to the 1:1 line, with a slope of 0.95 and $r^2 = 0.56$. A paired t-test analysis showed that mean PSSI values of the test and reference transects were not significantly different (P = 0.36). These results gave us confidence in the repeatability of the PSSI measurements.

Relating PSSI and Soil Properties

For the four small areas, possible relationships between PSSI and corresponding soil properties were investigated. Scatter plots did not indicate any clear non-linear relationships between pairs of the variables (Chung, 2004). Results of correlation analysis (table 1) showed a number of interactions among the soil properties. Bulk density and

Table 1. Correlations among PSSI and soil properties for the small 10 × 10 m areas.[a]

	BD (d.b., Mg m^{-3})	WC (d.b., %)	BD*WC (d.b., Mg m^{-3})	C (kN m^{-2})	ϕ (degrees)	Ca (kN m^{-2})	δ (degrees)	SF (fraction)	SiF (fraction)	CF (fraction)	PSSI (MPa)
WC	-0.83 (<0.01)										
BD*WC	-0.62 (<0.01)	0.95 (<0.01)									
C	0.34	0.05	0.23								
ϕ	0.53 (0.02)	-0.56 (0.01)	-0.48 (0.03)	-0.27							
Ca	0.38 (0.10)	-0.02	0.17	0.98 (<0.01)	-0.18						
δ	0.54 (0.01)	-0.55 (0.01)	-0.45 (0.05)	-0.16	0.98 (<0.01)	-0.04					
SF	0.42 (0.07)	-0.68 (<0.01)	-0.74 (<0.01)	-0.41 (0.07)	0.20	-0.43 (0.06)	0.09				
SiF	-0.09	0.30	0.41 (0.07)	0.45 (0.05)	0.14	0.54 (0.01)	0.30	-0.86 (<.01)			
CF	-0.68 (<0.01)	0.85 (<0.01)	0.80 (<0.01)	0.12	-0.60 (<0.01)	0.01	-0.64 (<0.01)	-0.63 (<0.01)	0.15		
PSSI	0.11	0.09	0.20	0.22	0.41 (0.08)	0.26	0.42 (0.06)	-0.37	0.43 (0.06)	0.06	
CI	0.48 (0.03)	-0.38 (0.10)	-0.27	0.15	0.59 (0.01)	0.22	0.61 (<0.01)	0.11	0.17	-0.47 (0.04)	0.69 (<0.01)

[a] BD = dry bulk density, WC = mass water content, BD*WC = volumetric water content, C = cohesion, ϕ = internal friction angle, Ca = adhesion, δ = soil-steel friction angle, SF = sand fraction, SiF = silt fraction, and CF = clay fraction. Numbers in parentheses are P values when the correlation coefficients are significant ($\alpha \leq 0.1$).

water content were significantly ($\alpha \leq 0.1$) correlated with each other as well as with laboratory-determined soil strength parameters (i.e., internal friction angle, soil-steel friction angle, and adhesion) and texture fractions. Significant correlations also existed among strength parameters and texture fractions.

Significant correlations with bulk density, water content, and clay fraction were not found for PSSI, but were found for CI. PSSI had significant positive correlations with internal friction angle, soil-steel friction angle, and silt fraction. Internal friction angle and silt fraction, however, showed significant correlations with several other soil properties. It should be noted that each variable used for the analysis included only a single value for each depth and texture area (n = 20). Results might improve if multiple measurements were taken at different depths and textures. Based on these results, we concluded that (1) bulk density, water content, strength parameters, and soil texture were related; (2) although the correlation data (table 1) did not show a significant relationship between PSSI and bulk density, water content, or their product (i.e., volumetric water content), the interrelationships between other variables suggested that such a relationship might emerge if more measurements were available; and (3) interactions among significant variables should be included along with the variables themselves in a model to predict PSSI.

Relating PSSI to CI, EC_a, Bulk Density, and Water Content

Figure 8 shows scatter plots of PSSI with respect to CI, EC_a, bulk density, and soil water content for three selected depths at the two field sites. Overall, PSSI vs. CI showed a

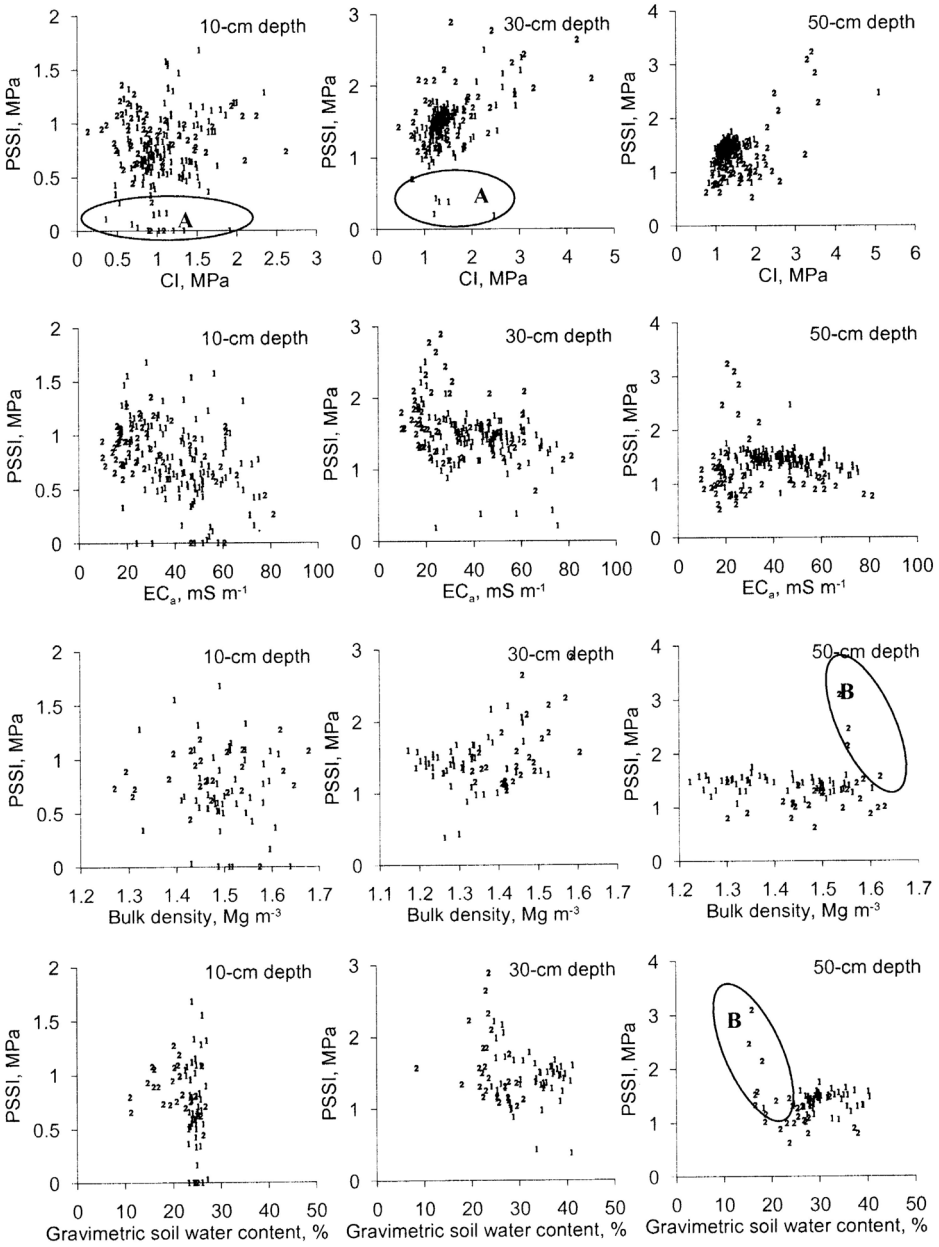

Figure 8. Scatter plots of PSSI with respect to CI, EC_a, dry bulk density and mass water content for different depths and field sites. Within each plot, the numbers 1 and 2 denote data from site 1 and site 2, respectively. Ellipses denoted by "A" and "B" are described in the text.

positive linear relationship, especially at the 30 cm depth. At the 10 cm depth, the patterns were not as clear and contained a number of possible outliers ("A" in fig. 8). These outliers were generally characterized by very small PSSI, likely due to unfavorable operational conditions (e.g., slotting, build-up of residue on the sensor) and lack of a full soil failure zone that affected the near-surface measurements. To automate removal of these questionable data points, the ratio of PSSI to CI was calculated, and the points where the ratio was more than two standard deviations away from the mean were considered to be outliers and removed before statistical analysis. This procedure removed more data at the shallower sensing depths (including most of the points identified in "A" in fig. 8) and very little at the greater depths (table 2). Although this filtering procedure achieved the desired effect in this situation, development of a more advanced filter should be considered as a topic for future research.

Generally, PSSI was higher with lower EC_a and soil water content, and greater bulk density values. The relationships between PSSI and EC_a were different, and of varying strength, for different sites, sensing depths, and EC_a ranges. For example, an overall trend of decreasing PSSI as a function of EC_a was seen at the 30 cm depth, with the greatest sensitivity of PSSI to changes in EC_a occurring where EC_a values were less than 40 mS m^{-1} (fig. 8). At the 50 cm depth, low-EC_a and high-PSSI locations also exhibited higher bulk density and lower water contents ("B" in fig. 8) than other locations. Descriptive statistics of the data (after outlier removal) used in the statistical analyses are summarized in table 2.

Correlations were calculated among PSSI, CI, and EC_a, and among sensor data and bulk density and water content (Chung, 2004). Correlations of EC_a, WC, and BD to PSSI and CI were significant for each site, with exceptions of PSSI and WC at site 2 and CI and WC at site 1. EC_a was negatively correlated to PSSI and CI for both sites. Patterns were similar when the data were grouped by depth, but significant correlations did not occur at all depths. For example, PSSI and WC were not significantly correlated at the 30, 40, and 50 cm depths for site 1 and at the 30 cm depth for site 2. When data were grouped by EC_a ranges, correlations between PSSI and EC_a, PSSI and WC, and PSSI and BD were often greater within one or more of the EC_a ranges than those for entire sites. However, statistical significance could not always be shown due to the reduced number of observations in the partial datasets. Compared with the correlations of EC_a, WC, and BD to PSSI, interactions between these soil properties showed higher significant correlation coefficients in many cases. For the entire dataset, EC_a and WC showed significant positive correlations, and WC and BD had significant negative correlations, for both sites. Correlation between EC_a and BD was not significant for site 1, but was for site 2.

Stepwise multiple linear regression was conducted to estimate PSSI as a function of CI, EC_a (as a surrogate for soil texture), bulk density (BD), and water content (WC), and quadratic and two-variable polynomial terms (e.g., BD^2, EC_a*WC). Table 3 shows the significant variables selected by the stepwise procedure to predict PSSI. The results confirmed that the effects of these variables on PSSI were different at different depths, EC_a ranges, and field sites. In site 2, water content and/or its interaction terms were significant at the 20 cm depth, while bulk density and/or its interaction terms were significant at the 30 cm depth. Significant variables were related to cone index and EC_a at the 50 cm depth in site 1, but to cone index and bulk density at the 30 cm depth in site 2. Better models ($R^2 \geq 0.9$ and RMSE ≤ 0.1) were obtained for site 1 at the 30 cm depth in a low EC_a zone, while for site 2 better models were obtained at the 20 and 40 cm depths in medium and high EC_a zones. In general, better models of PSSI were obtained when the data were divided into appropriate subgroups. In most but not all cases, grouping data by both depth and EC_a range produced better models with greater R^2 and/or smaller RMSE values with fewer model variables, compared with grouping by only depth or only EC_a range (table 3).

Adding depth and its interaction terms to the other candidate variables significantly improved the PSSI modeling (table 4). This agrees with the results given by Andrade-Sanchez et al. (2007), who also found it important to include depth in models relating soil strength data from a horizontally operating sensor to either BD and WC or to CI. Additionally, soil failure modeling has shown PSSI increases as a function of depth under an assumption of constant soil properties (Chung and Sudduth, 2006).

Most models for entire field areas and EC_a zones included variables related to sensing depth. For the entire sites, coefficients of determination increased to 0.66 for site 1 and

Table 2. Descriptive statistics for PSSI, CI, EC_a, dry bulk density (BD), and mass water content (WC) data obtained at the two field sites.

		Sensor Data							Soil Data				
	Depth	PSSI (MPa)		CI (MPa)		EC_a (mS m^{-1})[a]			BD (Mg m^{-3})		WC (%)		
	(cm)	Mean	SD	Mean	SD	Mean	SD	n[b]	Mean	SD	Mean	SD	n
Site 1	10	0.77	0.32	1.11	0.35	42.1	14.1	125	1.50	0.07	24.6	1.0	46
	20	1.04	0.36	1.62	0.53			130	1.44	0.11	28.1	4.9	51
	30	1.42	0.34	1.44	0.44			133	1.32	0.09	32.9	5.1	52
	40	1.68	0.26	1.31	0.31			132	1.37	0.08	32.4	4.1	52
	50	1.41	0.20	1.33	0.39			133	1.41	0.10	30.8	4.3	52
Site 2	10	0.85	0.21	1.10	0.51	31.5	19.1	43	1.46	0.10	20.2	4.6	22
	20	0.94	0.28	1.26	0.48			46	1.47	0.08	20.8	5.2	23
	30	1.63	0.47	1.76	0.81			47	1.45	0.08	23.8	4.7	23
	40	1.61	0.47	1.86	0.72			52	1.51	0.07	23.8	6.1	25
	50	1.25	0.60	1.79	0.71			52	1.50	0.09	23.7	6.1	25

[a] EC_a is a profile-weighted measurement, not a by-depth measurement.
[b] Number of observations remaining after outlier removal.

Table 3. Variables selected by stepwise multiple linear regression for the estimation of PSSI as a function of CI, EC_a, dry bulk density (BD), mass water content (WC), and quadratic and interaction terms, using experimental data obtained at two field sites.

	Site 1				Site 2			
Depth (cm)	Low (0-25)[a]	Medium (25-50)	High (50-76)	All (0-76)	Low (0-20)	Medium (20-40)	High (40-81)	All (0-81)
10	$CI*EC_a$ (0.32)[c] [0.33][d]	EC_a*WC CI (0.21) [0.29]	--[b]	EC_a*WC $CI*WC$ (0.3) [0.28]	$WC*BD$ WC^2 (0.82) [0.09]	--	--	EC_a^2 (0.18) [0.18]
20	$CI*BD$ (0.65) [0.22]	$CI*WC$ (0.1) [0.31]	EC_a*BD (0.31) [0.27]	$CI*WC$ $CI*EC_a$ (0.45) [0.30]	--	WC EC_a*BD (0.97) [0.04]	$CI*BD$ $CI*EC_a$ (0.99) [0.01]	EC_a*WC (0.44) [0.16]
30	CI^2 $WC*BD$ $CI*WC$ (0.98) [0.07]	$CI*WC$ (0.28) [0.21]	$CI*EC_a$ (0.47) [0.32]	CI^2 (0.28) [0.30]	$CI*EC_a$ BD^2 (0.69) [0.22]	BD CI^2 (0.98) [0.13]	BD^2 (0.50) [0.21]	$CI*BD$ BD^2 (0.57) [0.36]
40	$CI*WC$ (0.48) [0.20]	$CI*BD$ (0.31) [0.17]	$CI*EC_a$ (0.27) [0.21]	$CI*WC$ (0.17) [0.21]	CI (0.40) [0.30]	$CI*BD$ EC_a*WC BD (0.99) [0.05]	EC_a^2 $CI*BD$ (0.95) [0.04]	$CI*BD$ (0.79) [0.23]
50	$CI*EC_a$ (0.54) [0.15]	CI $CI*EC_a$ EC_a $CI*WC$ (0.64) [0.09]	--	CI $CI*EC_a$ EC_a CI^2 EC_a^2 $WC*BD$ (0.47) [0.11]	$WC*BD$ (0.42) [0.32]	CI^2 $CI*WC$ EC_a^2 EC_a (0.99) [0.06]	EC_a*BD (0.67) [0.15]	$WC*BD$ $CI*EC_a$ EC_a*BD BD^2 (0.72) [0.32]
All	$CI*WC$ BD^2 (0.55) [0.28]	$WC*BD$ $CI*WC$ $CI*EC_a$ (0.46) [0.32]	EC_a^2 (0.05) [0.42]	$CI*EC_a$ EC_a*BD WC^2 WC $CI*BD$ EC_a*WC $WC*BD$ CI^2 (0.46) [0.32]	$CI*WC$ BD^2 (0.42) [0.34]	$CI*BD$ $CI*WC$ (0.67) [0.42]	CI (0.47) [0.25]	$CI*BD$ CI $CI*WC$ (0.51) [0.37]

[a] Values in parentheses are ranges of EC_a values used to divide each field site into three textural classes.
[b] No variable met the 0.15 significance level for entry into the model.
[c] Values in parentheses are coefficients of determination, or R^2.
[d] Values in square brackets are RMSE (root mean square error) in MPa.

0.61 for site 2 (table 4), compared with 0.46 and 0.51 for the models without depth effects (table 3). When all data from the both field sites were used, a model that could explain 58% of the variability in PSSI was obtained. Better models, with larger R^2 and smaller RMSE values, were obtained in the low EC_a zone for site 1 and in the medium and high EC_a zones for site 2, where clay content was neither extremely low nor high. The best PSSI prediction (R^2 = 0.67) was found at the medium EC_a level in site 2 as a function of CI*BD and CI*WC (fig. 9).

PSSI prediction was also conducted using only EC_a, CI, and depth, along with their quadratic and two-variable polynomial terms as candidate independent variables. The purpose of this analysis was to determine if a relationship between PSSI and CI could be established without the need for collection of soil samples and subsequent laboratory analysis of WC and BD. Coefficients of determination of the selected models ranged from 0.47 to 0.64, slightly lower in some cases than those for models including bulk density and water content effects. In several cases, prediction of PSSI using only sensor data and depth was better than the prediction using all data (table 4) due to the larger number of data points available.

Table 4. Variables selected by stepwise multiple linear regression for the estimation of PSSI as a function of CI, EC_a, dry bulk density (BD), mass water content (WC), depth (De), and quadratic and interaction terms, using experimental data obtained at two field sites.

EC_a	Site 1			Site 2		
Range[a]	Model Variables	R^2	RMSE[b]	Model Variables	R^2	RMSE
Using sensor data and depth						
Low	CI, CI*EC_a, EC_a*De, De^2, CI^2	0.47	0.33	CI*De, De^2, De	0.53	0.31
Medium	De, De^2, CI*De, CI*EC_a, EC_a*De	0.64	0.26	CI	0.63	0.41
High	De, De^2, EC_a^2, EC_a, CI*EC_a, CI, CI^2	0.68	0.25	De, De^2, EC_a^2, CI*EC_a	0.57	0.24
All EC_a	CI*De, CI*EC_a, EC_a*De, De^2, De, EC_a^2, CI, EC_a	0.59	0.28	CI*De, De^2, De, EC_a^2, CI, CI*EC_a	0.64	0.33
Both sites	CI*De, EC_a^2, EC_a*De, De^2, De, CI*EC_a, EC_a, CI^2	0.56	0.31			
Using all data						
Low	CI*De, CI	0.65	0.25	CI*De, EC*BD	0.39	0.35
Medium	WC*De, CI*WC	0.55	0.29	CI*BD, CI*WC	0.67	0.42
High	WC*De, EC_a*WC, CI*De	0.55	0.30	CI	0.47	0.25
All EC_a	CI*EC_a, WC, EC_a*De, CI, De^2, De, EC_a*BD, EC_a^2, BD*De, CI^2, WC^2	0.66	0.26	CI*De, De^2, De, BD^2	0.61	0.34
Both sites	CI*De, WC^2, EC_a^2, EC_a*De, De^2, De, CI*EC_a, EC_a*BD, EC_a*WC	0.58	0.30			

[a] EC_a ranges of low, medium, and high were 0-25, 25-50, and 50-76 mS m^{-1} for site 1, and 0-20, 20-40, and 40-81 mS m^{-1} for site 2, respectively.
[b] RMSE = root mean square error of the regression (MPa).

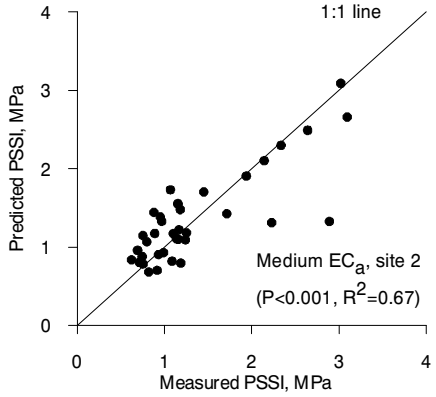

Figure 9. Scatter plot of predicted PSSI vs. measured PSSI for medium EC_a locations in site 2.

SUMMARY AND CONCLUSIONS

In our previous work (Chung et al., 2006), an on-the-go soil strength profile sensor (SSPS) was developed so that soil mechanical resistance could be measured at five depths simultaneously while traveling through agricultural fields. Force divided by the base area of the prismatic tip was defined as a prismatic soil strength index (PSSI). In this article, performance of the SSPS was evaluated using data obtained in a soil bin and two field sites with variations in soil water content, bulk density, and texture. The major findings were:

- In the soil bin, the SSPS was tested at three depths (10, 20, and 30 cm) and two compaction levels (high and low). When operating speed changed from 0.5 to 3.0 m s^{-1}, the increase in PSSI relative to the PSSI at the lowest speed level was less than 10% up to 2.0 m s^{-1}. When the SSPS was tested at three fixed speeds (0.5, 1.5, and 2.5 m s^{-1}), all three variables (speed, depth, and compaction level) had significant ($\alpha \leq 0.05$) effects on PSSI; however, there was not a significant difference in PSSI between 0.5 and 1.5 m s^{-1}. Compared with a 0.5 m s^{-1} speed, the increase in PSSI was about 2% at 1.5 m s^{-1} and 10% at 2.5 m s^{-1}. Because these results indicated that speed effects on PSSI would likely be minor below 1.5 m s^{-1}, we used this speed for field data collection.
- PSSI data at five depths (10, 20, 30, 40, and 50 cm) were collected in two fields with variations in bulk density, water content, and soil texture. Based on variogram analysis, data were averaged over a 4 m interval to remove measurement noise and small-scale variability. Kriged PSSI maps showed spatial and vertical variability in soil strength. PSSIs were generally higher in areas with lower EC_a values, corresponding to lower soil clay fractions.
- The repeatability of soil strength sensing with the SSPS was evaluated by comparing 4 m averaged PSSI measurements obtained from adjacent transects. The data from the two sets of transects matched well, being distributed around the 1:1 line.
- Correlation analysis relating PSSI to soil properties was conducted using data collected from four 10 × 10 m field areas selected for texture difference. PSSI showed significant ($\alpha \leq 0.1$) positive correlations with soil internal friction angle, soil-steel friction angle, and silt fraction. Significant correlations also existed among strength parameters and texture fractions. Bulk density and water content were not significantly correlated to PSSI, but were significantly correlated with each other and soil strength parameters (e.g., soil internal friction angle and adhesion) and texture fractions. This analysis indicated that interactions among bulk density, water content, and soil texture should be included in a model to predict PSSI.
- Effects of EC_a (as a surrogate for soil texture), bulk density, and water content on PSSI were investigated using data collected at five depths over entire field sites. Overall, PSSIs were higher at locations with lower EC_a (coarse texture) and water content (WC), and greater bulk

density (BD). Relationships between PSSI and soil properties were often different for different fields and depths.

- Results of stepwise multiple linear regression indicated that significant variables and their effects on PSSI were different in different depths, EC_a ranges, and field sites. Quadratic and interaction terms based on EC_a, BD, and WC were selected as significant variables in many cases, and better models were often obtained by dividing the data into appropriate subgroups based on depth or EC_a. Adding depth and its interaction terms as candidate independent variables significantly improved PSSI modeling. Coefficients of determination were 0.66 and 0.61 for the two field sites. Reasonably good PSSI predictions were obtained when only sensor data (i.e., CI and EC_a) were used as independent variables, with coefficients of determination only slightly lower than when bulk density and water content were also included in the model.

Overall, the prototype SSPS performed well, providing repeatable and stable measurements of soil strength in various soil and operating conditions. With its ability to acquire soil strength data at a high spatial and vertical resolution, the SSPS would be useful for a number of applications, e.g., delineation of compacted within-field areas and depths, assessment of variability in soil strength, and estimation of laboratory-determined soil properties (e.g., bulk density and water content).

ACKNOWLEDGEMENTS

This research was supported in part by the North Central Soybean Research Program, the United Soybean Board, and the International Cooperative Research Program, Rural Development Administration, Republic of Korea. The authors appreciate the assistance of Dr. John Bowders, Department of Civil Engineering, University of Missouri, in providing access to the direct shear testing device, and of Dr. Pedro Andrade, former graduate student in the Department of Biological and Agricultural Engineering, University of California-Davis, in soil sampling and field data collection.

REFERENCES

Adamchuk, V. I., M. T. Morgan, and H. Sumali. 2001. Application of a strain gauge array to estimate soil mechanical impedance on-the-go. *Trans. ASAE* 44(6): 1377-1383.

Alihamsyah, T., E. G. Humphries, and C. G. Bowers, Jr. 1990. A technique for horizontal measurement of soil mechanical impedance. *Trans. ASAE* 33(1): 73-77.

Anderson-Cook, C. M., M. M. Alley, J. K. F. Roygard, R. Khosla, R. B. Noble, and J. A. Doolittle. 2002. Differentiating soil types using electromagnetic conductivity and crop yield maps. *SSSA J.* 66(5): 1562-1570.

Andrade-Sanchez, P., S. K. Upadhyaya, and B. M. Jenkins. 2007. Development, construction, and field evaluation of a soil compaction profile sensor. *Trans. ASABE* 50(3): 719-725.

ASABE Standards. 2005a. S313.3. Soil cone penetrometer. St. Joseph, Mich.: ASABE.

ASABE Standards. 2005b. EP542. Procedures for using and reporting data obtained with the soil cone penetrometer. St. Joseph, Mich.: ASABE.

Ayers, P. D., and J. V. Perumpral. 1982. Moisture and density effect on cone index. *Trans. ASAE* 25(5): 1169-1172.

Canarache, A. 1991. Factors and indices regarding excessive compactness of agricultural soils. *Soil Tillage Res.* 19(2-3): 145-164.

Chukwu, E., and C. G. Bowers. 2005. Instantaneous multiple-depth soil mechanical impedance sensing from a moving vehicle. *Trans. ASAE* 48(3): 885-894.

Chung, S. O. 2004. On-the-go soil strength profile sensor. PhD diss. Columbia, Mo.: University of Missouri.

Chung, S. O., and K. A. Sudduth. 2006. Soil failure models for vertically operating and horizontally operating strength sensors. *Trans. ASABE* 49(4): 851-863.

Chung, S. O., K. A. Sudduth, and J. W. Hummel. 2006. Design and validation of an on-the-go soil strength profile sensor. *Trans. ASABE* 49(1): 5-14.

Elbanna, E. B., and B. D. Witney. 1987. Cone penetration resistance equation as a function of the clay ratio, soil moisture content, and specific weight. *J. Terramechanics* 24(1): 41-56.

Fredlund, D. G., and S. K. Vanapalli. 2002. Shear strength of unsaturated soils: Part 4. Physical methods. In *Methods of Soil Analysis*, 329-361. SSSA Book Series No. 5. J. H. Dane and G. C. Topp, eds. Madison, Wisc.: SSSA.

Gee, G. W., and D. Or. 2002. Particle-size analysis: Part 4. Physical methods. In *Methods of Soil Analysis*, 255-293. SSSA Book Series No. 5. J. H. Dane, and G. C. Topp, eds. Madison, Wisc.: SSSA.

Glancey, J. L., S. K. Upadhyaya, W. J. Chancellor, and J. W. Rumsey. 1989. An instrumented chisel for the study of soil-tillage dynamics. *Soil Tillage Res.* 14(1): 1-24.

Glancey, J. L., S. K. Upadhyaya, W. J. Chancellor, and J. W. Rumsey. 1996. Prediction of agricultural implement draft using an instrumented analog tillage tool. *Soil Tillage Res.* 37(1): 47-65.

Guerif, J. 1994. Chapter 9: Effects of compaction on soil strength parameters. In *Soil Compaction in Crop Production*, 191-214. B. D. Soane and C. Van Ouwerkerk, eds. Amsterdam, The Netherlands: Elsevier.

Hall, H. E., and R. L. Raper. 2005. Development and concept evaluation of an on-the-go soil strength measurement system. *Trans. ASAE* 48(2): 469-478.

Hettiaratchi, D. R. P., and A. R. Reece. 1967. Symmetrical three-dimensional soil failure. *J. Terramechanics* 4(3): 45-67.

Hettiaratchi, D. R. P., and A. R. Reece. 1974. The calculation of passive soil resistance. *Géotechnique* 24(3): 289-310.

Johnson, C. K., J. W. Doran, H. R. Duke, B. J. Wienhold, K. N. Eskridge, and J. F. Shanahan. 2001. Field-scale electrical conductivity mapping for delineating soil condition. *SSSA J.* 65(6): 1829-1837.

Kitchen, N. R., K. A. Sudduth, and S. T. Drummond. 1999. Soil electrical conductivity as a crop productivity measure for claypan soils. *J. Prod. Agric.* 12(4): 607-617.

Koolen, A. J., and H. Kuipers. 1983. *Agricultural Soil Mechanics.* Berlin, Germany: Springer-Verlag.

Lui, W., S. K. Upadhyaya, T. Kataoka, and S. Shibusawa. 1996. Development of a texture/soil compaction sensor. In *Proc. 3rd Intl. Conference on Precision Agriculture*, 617-630. P. C. Robert, R. H. Rust, and W. E. Larson, eds. Madison, Wisc.: ASA, CSSA, and SSSA.

Luth, H. J., and R. D. Wismer. 1971. Performance of plane soil cutting blades in sand. *Trans. ASAE* 14(2): 255-259, 262.

McKyes, E. 1985. *Soil Cutting and Tillage.* Amsterdam, The Netherlands: Elsevier.

Mulqueen, J., J. V. Stafford, and D. W. Tanner. 1977. Evaluating penetrometers for measuring soil strength. *J. Terramechanics* 14(3): 137-151.

Perumpral, J. V. 1987. Cone penetrometer applications: A review. *Trans. ASAE* 30(4): 939-943.

Plasse, R., G. S. V. Raghavan, and E. McKyes. 1985. Simulation of narrow blade performance in different soils. *Trans. ASAE* 28(4): 1007-1012.

Potyondy, J. G. 1961. Skin friction between various soils and construction materials. *Géotechnique* 11(4): 339-355.
Schuring, D. J., and R. I. Emori. 1964. Soil deforming processes and dimensional analysis. SAE Paper No. 897C. New York, N.Y.: SAE.
Soane, B. D., and C. Van Ouwerkerk. 1994. Chapter 1: Soil compaction problems in world agriculture. In *Soil Compaction in Crop Production*, 1-21. B. D. Soane and C. Van Ouwerkerk, eds. Amsterdam, The Netherlands: Elsevier.
Sojka, R. E., W. J. Busscher, and G. A. Lehrsch. 2001. In situ strength, bulk density, and water content relationships of a Durinodic Xeric Haplocalcip soil. *Soil Sci.* 166(8): 520-529.
Stafford, J. V. 1979. The performance of a rigid tine in relation to soil properties and speed. *J. Agric. Eng. Res.* 24(1): 41-56.
Sudduth, K. A., N. R. Kitchen, G. A. Bollero, D. G. Bullock, and W. J. Wiebold. 2003. Comparison of electromagnetic induction and direct sensing of soil electrical conductivity. *Agron. J.* 95(3): 472-482.
Sudduth, K. A., J. W. Hummel, and S. T. Drummond. 2004. Comparison of the Veris Profiler 3000 to an ASAE-standard penetrometer. *Applied Eng. in Agric.* 20(5): 531-541.
Sudduth, K. A., N. R. Kitchen, W. J. Wiebold, W. D. Batchelor, G. A. Bollero, D. G. Bullock, D. E. Clay, H. L. Palm, F. J. Pierce, R. T. Schuler, and K. D. Thelen. 2005. Relating apparent electrical conductivity to soil properties across the north-central USA. *Comp. Elect. Agric.* 46: 263-283.
Taylor, H. M., and H. R. Gardner. 1963. Penetration of cotton seedling taproots as influenced by bulk density, moisture content, and strength of soil. *Soil Sci.* 96(3): 153-156.
Van Bergeijk, J., D. Goense, and L. Speelman. 2001. Soil tillage resistance as tool to map soil type differences. *J. Agric. Eng. Res.* 79(4): 371-387.
Webster, R., and M. A. Oliver. 1990. *Statistical Methods in Soil and Land Resource Survey.* New York, N.Y.: Oxford University Press.
Wells, L. G., and O. Treesuwan. 1978. The response of various soil strength indices to changing water content and bulk density. *Trans. ASAE* 21(5): 854-861.
Wheeler, P. N., and R. J. Godwin. 1996. Soil dynamics of single and multiple tines at speeds up to 20 km/h. *J. Agric. Eng. Res.* 63(3): 243-250.
Wismer, R. D., and H. J. Luth. 1972. Performance of plane soil cutting blades in clay. *Trans. ASAE* 15(2): 211-216.
Zhang, B., Q. G. Zhao, R. Horn, and T. Baumgartl. 2001. Shear strength of surface soil as affected by soil bulk density and soil water content. *Soil Tillage Res.* 59(3-4): 97-106.